SSRG International Journal of Civil Engineering
ISSN: 2348-8352/ https://doi.org/10.14445/23488352/IJCE-V13I7P117

Volume 13 Issue 7, 262-275, July 2026

Original Article

Influence of Reinforced Concrete Wall Mesh Size on Seismic Response and Its Relationship with Building Height

Heydi Karina Hinostroza Maravi[1], Erick Oswaldo Gamboa Tolentino[2], Lileana Carolina Saavedra Robles[3]

[1]*School of Engineering, Universidad Continental, Huancayo, Peru.*
[2]*Department of Civil Engineering, National University of Engineering, Lima, Peru.*
[3]*Department of Architecture, Autonomous University of Guayaquil, Ecuador.*

[1]*Corresponding Author : 70345903@continental.edu.pe*

Received: 03 May 2026 Revised: 25 June 2026 Accepted: 03 July 2026 Published: 29 July 2026

Abstract - *The modeling of reinforced concrete walls in ETABS may be influenced by the mesh size adopted in the model. In this regard, the present study evaluates the influence of mesh size and its relationship with building height. The objective is to analyze the combined effect of meshing and height and to assess their influence on global and local parameters of the structural response. For this purpose, the seismic design of a 15-story building was performed in accordance with Standard E.030, after which the height was progressively varied down to 5 stories, resulting in a total of 11 models. In all models, the walls were discretized using mesh sizes of 1 m, 0.8 m, 0.6 m, 0.4 m, and 0.2 m, and the results were obtained from modal response spectrum dynamic analysis. The results showed that, as the mesh size decreases, interstory drifts and vibration periods progressively increase, with a greater influence observed in the taller models. For base shear, the variations were smaller, although increasing or decreasing trends were observed depending on the analysis direction, particularly in models taller than 10 stories. Regarding the internal forces in the walls, axial forces and bending moments exhibited greater changes with finer meshing compared with shear forces.*

Keywords - *Base Shears, Interstory drifts, Etabs, Internal forces in walls, Wall meshing.*

1. Introduction

Currently, the seismic analysis of buildings is performed using specialized programs, with an increase in their use as computational progress advances and due to the need to model increasingly complex structures. One of the most widely used software programs is ETABS, which allows the analysis of structural models in two and three dimensions, as well as the design of their elements, according to the design codes of different countries [1]. Likewise, the results depend on how the modeling of such structural elements is considered within the software. One of these elements is shear walls, since they can resist lateral loads that contribute to controlling horizontal displacements in medium- and high-rise buildings, an important factor for the control of drifts established by seismic regulations [1]. In ETABS, shear walls can be represented as membrane-type or shell-type area elements. The membrane element has three degrees of freedom per node, according to the behavior within its plane, so it does not consider deformation outside it. Load distribution is carried out through tributary areas, transferring them to the elements that do contribute stiffness to the system. On the other hand, the shell element has six degrees of freedom per node. This allows it to represent axial, shear, and flexural deformations and to contribute stiffness both within and outside its plane. Due to this, the shell element is the most commonly used for modeling shear walls, because of its ability to represent their behavior more completely, although the definition of its edges must be considered, as well as a uniform and proportional mesh, since this can vary the results of stresses and deformations [2, 3].

Although shear walls can be represented as area elements, they may also have other types of modeling considerations. In this regard, Chelariu et al. [4] compared the errors that may occur in the idealization of walls. As a first case, they analyzed a solid wall, representing it as a fixed bar, an unmeshed shell-type element, and a sufficiently meshed element, comparing them in terms of displacement. The unmeshed wall can generate errors greater than 30%, although a refined model is recommended in an analysis where displacements are relevant. In a second case, they evaluated walls with superimposed openings, representing them as equivalent frames, with meshed and unmeshed shell elements. They evaluated maximum displacements, axial force, and overturning moments as a function of the degree of coupling. As in the first case, a similar trend was observed, indicating that the results depend on the type of idealization and the adopted discretization, with the discretized model being the one that best represents the behavior of the wall. For his part, Rusi [5] evaluated shear walls idealized as bar-type elements with rigid arms, shell elements as plates with boundary elements, and plates only. The comparison was carried out based on natural vibration periods, displacement, internal forces in the wall, vertical forces, and stresses at the bases, concluding that modeling the walls with columns provides a better representation.

In addition, they compared the effect of wall meshing by formulating divisions of 1x1, 5x1, 5x4, and 10x8, to evaluate its influence on the structural response and select a reasonable mesh. As the mesh was refined, the periods and displacements increased slightly, while the differences in internal forces were small. Therefore, excessive mesh refinement does not produce significant changes, but it does increase the complexity of the model and the calculation time. On the other hand, according to what is cited in the study, the mesh size can be approximately adopted as 1/3 to 1/4 of the story height.

On the other hand, other parameters, such as the type of diaphragm in slabs, the rigid arm factor, as well as the meshing of shear walls, were evaluated simultaneously to assess their influence on the model. Paitán et al. [2] evaluated a 10-story building by varying these parameters as their main objective. Among their results, they showed that modeling with a membrane type, a rigid arm of 0.5, and manual meshing presented better global behavior in terms of displacement, stiffness, shear force, overturning moment, and interstory drift values. It also indicates that automatic wall meshing can produce losses in deformation and stress when flexible elements are used. In the case of manual meshing, it allows better control and a more adequate representation of the wall behavior. In addition, excessive meshing in walls with low slenderness can generate more flexible behavior. In the case of taller walls, increasing the meshing produces minimal changes in the response, indicating that, for a certain level of meshing, further refinement no longer generates improvements in analysis accuracy.

Because analysis in structural design software seeks to represent the behavior that a structure will have, evaluating how close the results are to reality is one of the aspects to consider guaranteeing the reliability of the results. Mangan et al. [6] developed a computational model of the Kennedy Library, with the objective of determining the modal parameters and comparing them with the results obtained through tests and analyzing how closely the model approaches real conditions. The authors showed that the model calibration process not only required considering cracked properties of walls and slabs, as well as diaphragm stiffness, but also the meshing of these elements, since representing a wall with elements that are too large can overestimate its stiffness due to the low representation of deformations.

Although the previous studies evaluated reinforced concrete walls, research has also been conducted on confined masonry walls. Luna et al. focused on studying maximum displacements and shear stresses in isolated walls and in a five-story building, considering meshes of 1, 2, 4, 8, 16, and 32 divisions per edge. They concluded that eight elements per edge were sufficient to obtain reliable results and that further refinement only increased the computational cost. On the other hand, they observed that meshing had a greater influence on the distribution of stress than on the global displacements [7].

According to the reviewed literature, establishing a mesh size usually depends on factors such as the geometry of the element, the height of the Building, and the required level of accuracy. However, in professional practice, a mesh size is often adopted based on common criteria, without sufficiently verifying its effect on the structural response [2]. Several studies have shown that as this size changes, analysis results such as displacements, vibration periods, stress distribution, internal forces, and stress distribution in the walls may be modified. Nevertheless, the available evidence has been limited, since some studies usually analyze the results obtained in particular cases, such as the type of idealization of shear walls, or evaluate the changes in a building with a specific height, which does not allow observing whether the variation in mesh size generates significant changes in the seismic response as the height of the building changes.

In this context, the present study aimed to evaluate the sensitivity of the meshing of reinforced concrete walls in ETABS on the results of drifts, base shears, and internal forces in the walls, as the height of the building changes. For this purpose, the modeling and seismic analysis of a 5-story base building was developed, from which higher-height models were generated until reaching 15 stories, while keeping the other element properties and modeling considerations constant, in order to evaluate the variations in the results only in terms of mesh size and building height. In addition, in each case, different mesh sizes of 1 m, 0.8 m, 0.6 m, 0.4 m, and 0.2 m were evaluated, as well as how much the results change as a function of such discretization and height.

This study focused on these two factors because shear walls provide the greatest contribution to lateral stiffness against displacements, and a change in the mesh makes these elements more flexible, modifying the global response of the structure. In addition, as the building height increases, the fundamental period and displacements also become more sensitive to larger changes. Although the seismic response is influenced by various factors, such as structural configuration, material properties, among other factors, seismic analysis is performed based on the global response of the structural model, to obtain the demand force on each structural element before design. In this regard, parameters such as the vibration period reflect the global stiffness of the system and condition the seismic demands, from which lateral displacements are generated. These are evaluated through drifts and must remain within the admissible limits established by the code. Likewise, this change is reflected in the base shear, which in turn may change the stiffness contribution of the shear walls, as well as the distribution of their internal forces.

2. Materials and Methods

To the analysis, the present study considered an arbitrary location for the Building, since only the analysis of the variation in the results will be performed for comparative purposes according to the change in mesh size and building height.

In this regard, the Building was established in an area of the district of El Tambo, province of Huancayo, department of Junín, for the definition of the seismic parameters. It should be noted that, based on these considerations, the structural configuration and preliminary sizing were carried out to comply with the drift requirements according to the E.030 code. In addition, this study is developed with a quantitative approach, of an applied type, with an explanatory level and a non-experimental design.

2.1. Materials

2.1.1. Structural Model

The model used corresponds to a 15-story reinforced concrete office building, with a total height of 42 m, a story height of 2.8 m, and a total area of 301.69 m². From this base model, additional models will be generated by progressively reducing one story at a time down to 5 stories, resulting in a total of 11 models that vary only in height while maintaining a regular floor plan. The structural system consists of columns and walls. The latter are distributed at the edges of the floor plan, in the central area, and around the elevator core, as shown in Figure 1. In addition, Figure 2 shows a three-dimensional view of the structure.

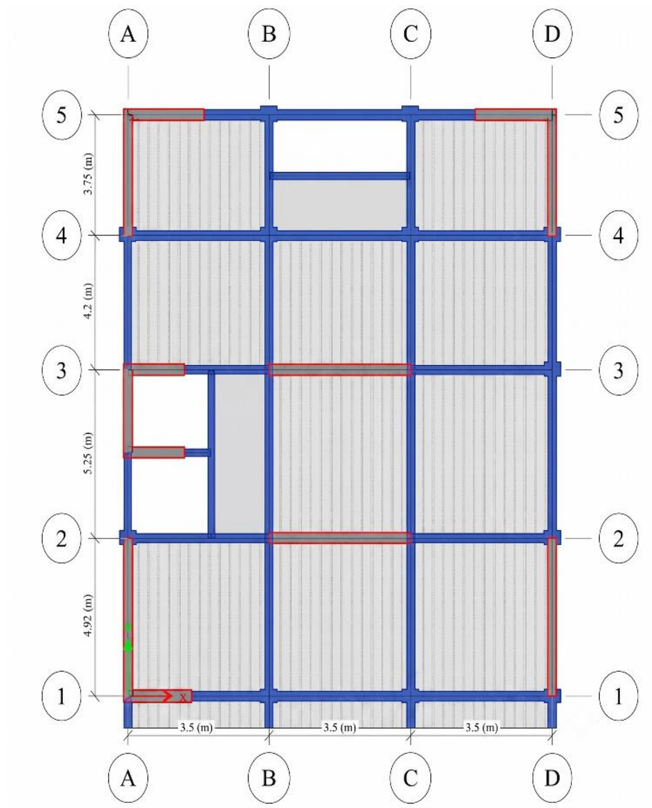

Fig. 1 Plan distribution of the structural model

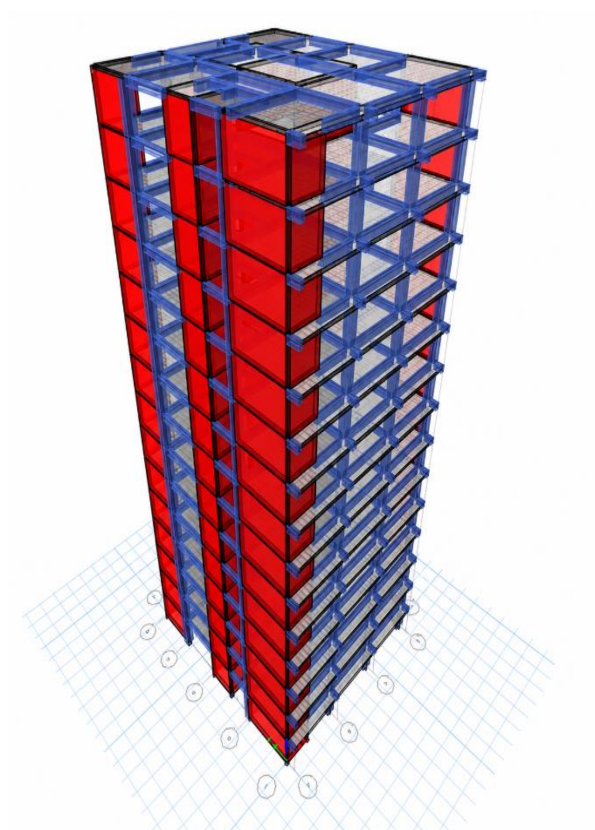

Fig. 2 Three-dimensional model

2.1.2. Software ETABS Versión 22.5.1

ETABS will be used for the seismic modeling and analysis of the Building. This program is a structural analysis and design software package specifically focused on buildings and is used for both simple and complex structures. The program allows the structure to be defined in terms of stories, grids, bays, and construction elements, thereby facilitating modeling.

Likewise, it integrates the distribution of gravity loads, seismic and wind loads, and linear and nonlinear analysis based on finite elements. In addition, it enables the design of concrete and steel elements, composite elements, and connections. The results obtained include reactions and forces in the elements, vibration modes, nodal and story displacements, story shears, and drifts, with graphical visualization of results, as well as report generation, among others [1].

2.2. Analysis Method

The seismic analysis of the Building was performed in accordance with Standard E.030 Seismic-Resistant Design, and Standard E.060 Reinforced Concrete was used for the characterization of the materials. The adopted concrete properties include a compressive strength of $f'c = 280\ kg/cm^2$ and an elastic modulus of $E_c = 15100\sqrt{f'c}$, Grade 60 steel was considered, with a yield strength of $f'c = 4200\ kg/cm^2$ and an elastic modulus of $E_c = 2000000\ kg/cm^2$. On the other hand, the dimensions of the structural elements are presented in Table 1, while the seismic parameters are shown in Table 2.

Table 1. Dimensions of the structural elements

Elements	Dimensions (cm)
Column	C1 = 50 x 70
Beams	V1 = 25 x 45
	V2 = 30 x 40
	V3 = 30 x 50
Ribbed Slab	e = 20
Solid Slab	e = 15
Walls	e = 35

Table 2. Seismic parameters

Seismic Parameters	Coefficients
Zone Factor "Z"	0.35
Use Factor "U"	1
Soil Factor "S"	1.15
Seismic Amplification Factor	1.607
Basic Reduction Coefficient "R0"	6
Ia	1
Ip (torsional irregularity)	0.75

The concrete walls and slabs were modeled as shell-type area elements; therefore, to ensure better load transfer, the same mesh size was used for both elements. Accordingly, each model will be analyzed using square mesh sizes of 0.2 m, 0.4 m, 0.6 m, 0.8 m, and 1 m. Table 3 presents the cases of the analyzed models, and Figure 3 shows the application of internal meshing to the wall along axis 2.

Table 3. Cases of the analyzed models

N°	Model	N° of stories	Mesh size
01	M15	15	(1 m, 0.8 m, 0.6 m, 0.4 m, 0.2 m)
02	M14	14	
03	M13	13	
04	M12	12	
05	M11	11	
06	M10	10	
07	M09	9	
08	M08	8	
09	M07	7	
10	M06	6	
11	M05	5	

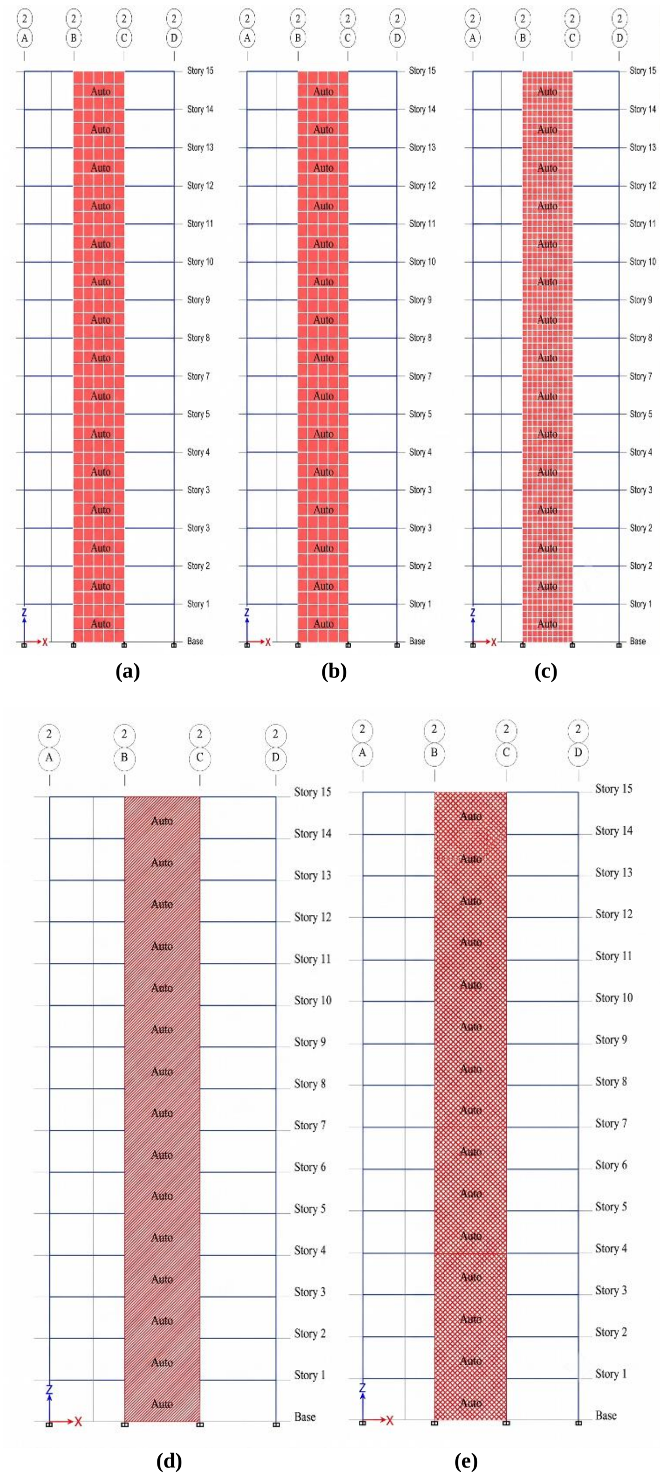

Fig. 3 Internal meshing of the wall along axis 2 with different mesh sizes: (a) 1 m, (b) 0.8 m, (c) 0.6 m, (d) 0.4 m, (e) 0.2m.

This meshing range was adopted to analyze the sensitivity of the structural response as the mesh is refined. According to the study cited by Rusi, a mesh size of 1/3 or 1/4 of the story height is proposed [5]. In this case, given the story height of 2.8 m, the mesh size would range between 0.7 m and 0.93 m;

therefore, 1 m was adopted as the reference size. In addition, the software establishes a default size of 1.2192 m for the internal discretization of shell elements, both for slabs and walls.

Likewise, as mentioned above, the mesh sizes used may vary; however, in practice, values within the range of 0.4 m to 0.6 m are commonly adopted. Based on the finite element convergence criterion, the mesh should be refined until the stability of the results is verified, and a balance between result accuracy and computational cost is achieved. However, in high-rise structures dominated by walls, the computational time is considerably greater, since the software must analyze a large number of elements. For this reason, a minimum mesh size of 0.20 m was considered.

The parameters analyzed were interstory drifts, vibration periods, and base shear, which represent the global response of the Building to seismic actions. In addition, the internal forces of two representative walls were evaluated for each analysis direction, including axial forces, shear forces, and bending moments, since these results influence the structural design of the elements.

2.2.1. Interstory Drifts

Interstory drift is obtained by dividing the relative displacement between two consecutive stories by the height of the corresponding story. It is a demand parameter and an indicator of structural performance that is correlated with damage to structural and nonstructural components [8]. Standard E.030 establishes that, for regular structures, lateral displacements are calculated by multiplying the results of the linear elastic analysis by 0.75R, whereas for irregular structures, they are multiplied by 0.85R. Based on these displacements, relative interstory displacements can be obtained and compared with the maximum limit established by the Standard, which is 0.007 for reinforced concrete structures and must not be exceeded [9].

2.2.2. Fundamental Period of Vibration

The natural period of vibration is the time required for a structure to complete one cycle of free vibration. In systems with multiple degrees of freedom, each mode of vibration is associated with a corresponding natural period [10]. For the static analysis established in Standard E.030, these values can be obtained from expressions that depend on variables such as height and structural system. However, for modal response spectrum analysis, the Standard indicates that the vibration modes must be determined using a procedure that adequately represents the stiffness and mass distribution. Furthermore, it specifies that the sum of the effective modal masses must be at least 90% of the total mass in each direction of analysis [9].

2.2.3. Base Shear

This parameter represents the total lateral force at the base of the structure. According to Standard E.030, in static analysis, it is determined based on a coefficient that depends on factors such as the zone factor, use factor, soil factor, reduction coefficient R, and seismic weight, which in turn depends on the total weight of the structure and a percentage of the live load or imposed load.

For modal response spectrum dynamic analysis, the base shear values are obtained from the inelastic pseudo-acceleration spectrum, derived from the seismic coefficient and gravity; therefore, the base shears are obtained from modal analysis and modal combination. In addition, it must be verified that the dynamic base shear is at least 80% of the static base shear for regular structures and 90% for irregular structures. If this requirement is not met, the forces are proportionally scaled, except for displacements [9].

2.2.4. Distribution of Internal Forces in Walls

In the design of concrete walls, axial force, shear force, and bending moment are the load demands for which it must be verified whether the capacity of the element is sufficient to resist them. These values are obtained from the software, depending on the load combination case evaluated. However, for comparison purposes, these results were obtained from the modal response spectrum analysis for each analysis direction.

Axial Force

It is the force that acts along the axis of the element, produced by transmitted gravity loads, the self-weight of the element, dead loads, and live loads. In the seismic response, this force may vary depending on the global behavior of the Building, resulting in an increase or reduction in compression and even tension under certain load combinations. In design, the axial force is analyzed together with the bending moment to verify the P–M interaction [11].

Bending Moment

It is the load effect that produces wall curvature induced by lateral forces, generating compression and tension zones within the section [11]. In addition, depending on the magnitude of the force demand, the need for boundary elements is defined; these depend on the magnitude of compression or tension acting on the element and on the neutral axis depth obtained from the analysis [12].

Shear Force

It is associated with lateral loads and is important because shear failure is more brittle than flexural failure. In the case of squat walls, shear strength may govern the response, whereas in slender walls, flexure controls the behavior [11].

3. Results and Discussion

3.1. Interstory Drifts

The following section presents the trend of interstory drifts as the mesh size changes in both the X and Y directions. Graphically, the results are shown for the 15-story and 5-story buildings, considering that these represent the tallest and shortest cases, respectively.

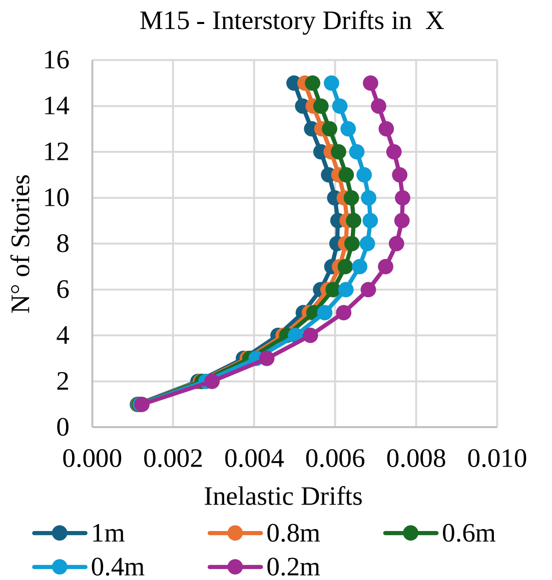

Fig. 4 Interstory drifts in the X direction for the 15-story building

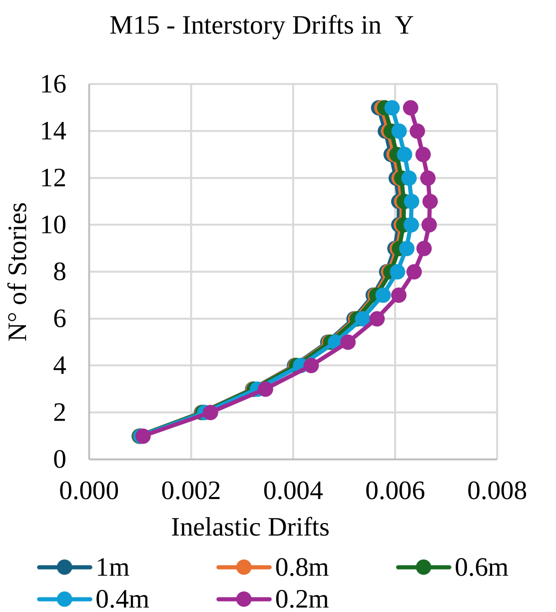

Fig. 5 Interstory drifts in the Y direction for the 15-story building

As shown in Figures 4 and 5, when a mesh size between 1 m and 0.6 m is considered, the differences in the increase in drifts are slight compared with the 0.4 m and 0.2 m meshes, with the latter showing the greatest difference. In the X analysis direction, the change is more significant, with a variation of 37.81% between the 0.20 m mesh and the 1.0 m mesh, whereas in the Y direction, the variation is 11.06%. This difference shows that, although the same discretization is used in both directions, the response sensitivity differs. This may be associated with the structural configuration and stiffness distribution provided by the walls, since their location and symmetry influence the lateral response, including displacements and drifts [13]. Moreover, as shown in Table 2, the model presents torsional plan irregularity. Therefore, this effect is another aspect that may influence the global response of the structure, causing the structural configuration not to respond in the same way in plan [14].

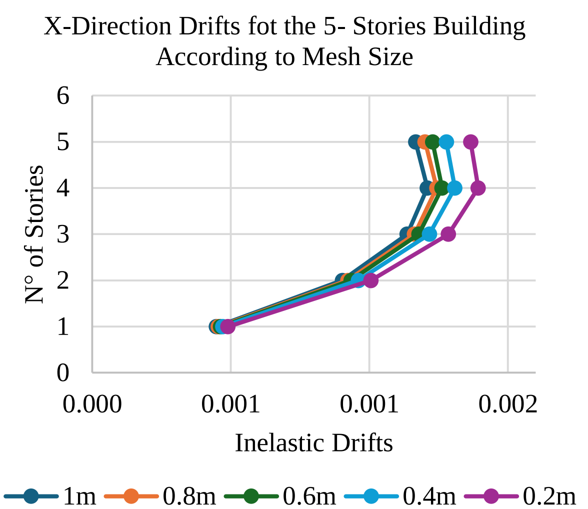

Fig. 6 Interstory drifts in the X direction for the 5-story building

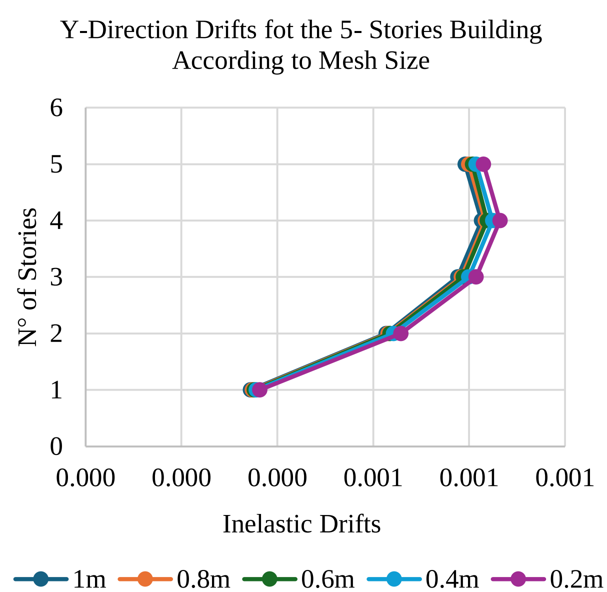

Fig. 7 Interstory drifts in the Y direction for the 5-story building

For the 5-story Building, as shown in Figures 6 and 7, the trend is similar to that obtained for the 15-story model, although with different variations. Although a greater increase in drifts is observed in the X direction, as shown in Figure 6, it reaches only a variation of 17.05% for the 0.2 m mesh relative to the 1 m mesh. In the Y direction, this variation was only 4.83%.

Although the drift results for the two previously discussed cases were presented graphically, the analysis was performed for all model cases. Table 4 presents the maximum drift variations in both directions.

Table 4. Maximum drift variation for the 0.20 m mesh relative to the 1.00 m mesh

Model	X Direction	Y Direction
M15	37.81%	11.06%
M14	36.05%	11.20%
M13	33.51%	11.23%
M12	31.04%	10.91%
M11	28.54%	13.13%
M10	35.70%	11.21%
M09	37.01%	10.38%
M08	32.20%	9.16%
M07	27.20%	7.86%
M06	22.00%	6.58%
M05	17.05%	4.83%

As shown in Table 4, the variations change according to the analysis direction and building height. In the X direction, the largest variations are observed, ranging from 17.05% for the 5-story model to 37.81% for the 15-story model.

In general, slight changes are observed among the model results as the height decreases, following a reduction in variation from the 15-story to the 11-story model, an increase in the 11- to 9-story models, and, from that point onward, a progressive reduction.

The variations in the Y direction range from 4.83% to 11.06%. The trend is similar to that of the other direction, but with a slight increase from the 15-story to the 12-story model, an increase in the 11-story model, and, from that point onward, a reduction.

The results suggest that a smaller mesh size has a greater influence on buildings of considerable height. This is because, as height increases, demand increases due to lateral effects, and from approximately 10 stories onward, stiffness governs more than strength, since displacements increase with height [15]. In addition, as the mesh is further refined, a longer computational time is required due to the fineness of the mesh [2].

3.2. Fundamental Period of Vibration

Table 5 presents the periods of the first three vibration modes, with mode 1 predominantly corresponding to translation in the X direction, mode 2 to translation in the Y direction, and mode 3 to rotation. These results correspond to all the models analyzed as a function of the variation in mesh size.

Table 5. Vibration periods, in seconds, of the first three modes according to mesh size

Mod	Mode	1m	0.8m	0.6m	0.4 m	0.2m
M15	1	1.008	1.025	1.037	1.069	1.151
	2	0.916	0.926	0.932	0.943	0.960
	3	0.625	0.632	0.637	0.647	0.670
M14	1	0.914	0.929	0.941	0.969	1.042
	2	0.826	0.834	0.839	0.849	0.863
	3	0.565	0.571	0.575	0.584	0.604
M13	1	0.822	0.836	0.846	0.872	0.935
	2	0.738	0.745	0.749	0.757	0.769
	3	0.506	0.511	0.515	0.523	0.539
M12	1	0.732	0.744	0.754	0.776	0.830
	2	0.653	0.658	0.662	0.668	0.678
	3	0.449	0.453	0.456	0.463	0.477
M11	1	0.645	0.656	0.664	0.683	0.729
	2	0.570	0.575	0.577	0.582	0.590
	3	0.393	0.397	0.399	0.405	0.416
M10	1	0.560	0.570	0.577	0.593	0.630
	2	0.491	0.494	0.496	0.500	0.506
	3	0.339	0.343	0.345	0.349	0.358
M09	1	0.479	0.487	0.493	0.506	0.535
	2	0.415	0.418	0.419	0.422	0.426
	3	0.288	0.291	0.292	0.296	0.303
M08	1	0.401	0.408	0.412	0.423	0.444
	2	0.343	0.345	0.346	0.348	0.352
	3	0.240	0.242	0.243	0.245	0.250
M07	1	0.327	0.332	0.336	0.343	0.358
	2	0.277	0.278	0.279	0.280	0.282
	3	0.194	0.196	0.196	0.198	0.202
M06	1	0.258	0.262	0.264	0.269	0.279
	2	0.215	0.216	0.217	0.218	0.219
	3	0.152	0.153	0.154	0.155	0.157
M05	1	0.194	0.197	0.198	0.201	0.207
	2	0.161	0.161	0.161	0.162	0.163
	3	0.114	0.115	0.115	0.116	0.117

As shown in Table 5, the periods progressively increase as the mesh size decreases, suggesting a reduction in the structural stiffness. This trend is consistent with that observed for the drifts, since both parameters are influenced by the global stiffness of the Building; as the mesh is refined, the structure becomes more flexible. In addition, the periods vary according to the height of the model, the distribution of walls in each direction, the plan aspect ratio, the polar moment of inertia, and torsion [16]. Tall buildings have longer periods, which are reflected in significant displacements [17]. On the other hand, the variation in periods between the 0.20 m and 1 m meshes becomes smaller for models with fewer stories. For the 15-story model, this variation is 14.19% for mode 1, 4.80% for mode 2, and 7.20% for mode 3, whereas for the 5-story model, the variation is smaller, with values of 6.70%, 1.24%, and 2.63%, respectively. The difference in these percentages remains greater in the X direction than in the Y direction.

3.3. Base Shear

Table 6 presents the base shears obtained from the modal response spectrum seismic analysis for the X and Y analysis directions, as well as for the different mesh sizes evaluated. These results allow the changes in global seismic demand to be assessed and make it possible to analyze whether the results follow trends similar to those observed for interstory drifts and vibration periods.

Table 6. Base shear, in tons, according to mesh size

Mod	Vb	1m	0.8m	0.6m	0.4m	0.2m
M15	X	481.95	475.49	471.70	465.55	451.27
	Y	474.05	476.59	478.49	484.95	495.64
M14	X	487.04	480.72	476.84	469.81	456.13
	Y	483.40	486.52	488.72	495.55	506.28
M13	X	494.69	488.85	485.15	478.02	462.17
	Y	496.27	499.84	502.21	508.99	518.98
M12	X	505.51	500.05	496.42	488.92	472.12
	Y	513.93	517.77	520.18	526.65	535.61
M11	X	514.96	511.68	508.88	502.01	485.45
	Y	513.92	519.87	523.76	532.94	547.21
M10	X	494.42	499.57	502.74	510.45	522.45
	Y	476.32	481.22	484.27	491.07	501.13
M09	X	448.58	453.03	455.68	461.82	471.09
	Y	434.60	438.69	441.18	446.52	454.47
M08	X	402.84	406.42	408.51	413.15	420.01
	Y	392.53	395.76	397.68	401.66	407.56
M07	X	356.75	359.43	360.97	364.27	369.09
	Y	349.75	352.13	353.54	356.36	360.55
M06	X	309.94	311.81	312.87	315.07	318.23
	Y	305.94	307.59	308.57	310.46	313.28
M05	X	262.14	263.34	264.04	265.39	267.29
	Y	260.86	261.94	262.59	263.79	265.57

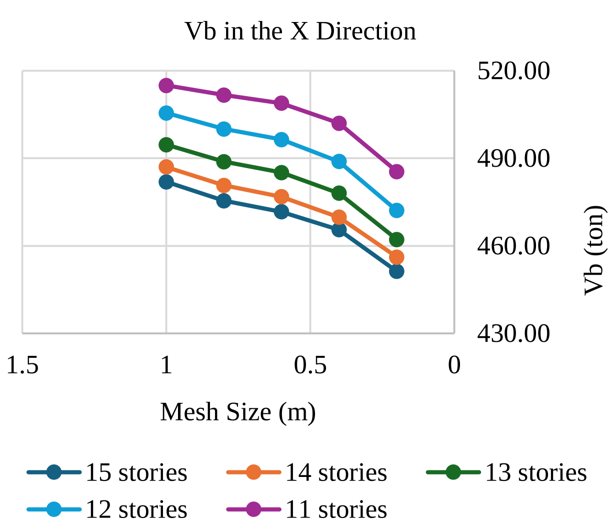

Fig. 8 Base shear in the X direction according to mesh size for the 15- to 11-story models

The influence of meshing on base shear in the X direction does not show a uniform trend across all the analyzed models, as shown in Figures 8 and 9. For the 15- to 11-story models, as the mesh size decreases, the base shear also decreases, reaching variations between the 0.2 m mesh and the 1 m mesh of 6.37%, 6.35%, 6.57%, 6.61%, and 5.73% for the 15-, 14-, 13-, 12-, and 11-story models, respectively.

According to Figure 9, from the 10-story to the 5-story models, the change in base shear caused by mesh refinement is related to the behavior observed for drifts and periods, showing a progressive increase. The variations between the 0.2 m and 1 m meshes are 5.67%, 5.02%, 4.26%, 3.46%, 2.67%, and 1.96% for the 10-, 9-, 8-, 7-, 6-, and 5-story models, respectively. Based on these results, the influence of meshing on the response decreases as the building height decreases.

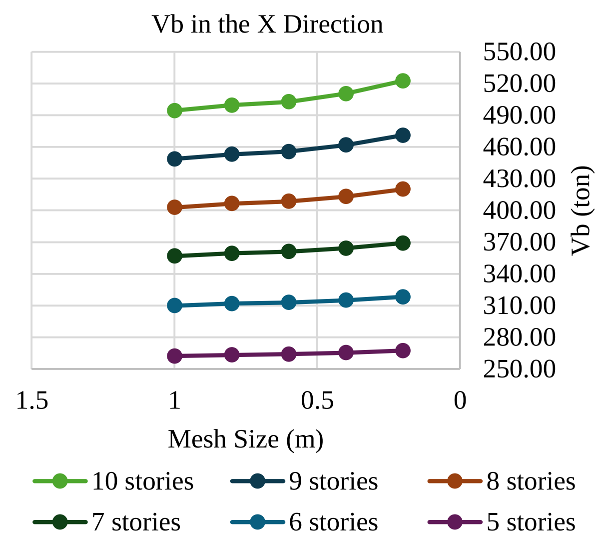

Fig. 9 Base shear in the X direction according to mesh size for the 10- to 5-story models

In modal response spectrum dynamic analysis, base shear is obtained from the combined modal response of the structural system, considering vibration modes, effective masses, and response combination. In the X and Y analysis directions, Standard E.030 incorporates an inelastic pseudo-acceleration spectrum, causing the spectral demand to depend partly on a given period [9]. Based on this, an increase in the period, which is what occurs as the mesh size decreases, does not necessarily imply that the base shear must decrease, since the response depends on the period reached. In this case, the analysis considers an S2 with Tp = 0.6 s, which is the limit at which seismic amplification remains constant; beyond this point, it begins to decrease. In this regard, according to Table 5, all mode 1 periods from the 11-story model onward are greater than this value, which explains this increase. Unlike the previous case, the base shear results in the Y direction increased for the 11- to 15-story models, despite having a modal period greater than Tp. This suggests that the response cannot be interpreted solely based on the modal period, but rather on the complete modal combination. However, base shear is verified according to Standard E.030, ensuring that it reaches a minimum of 80% of the static base shear for regular structures and 90% for irregular structures. This requires the values to be scaled for design purposes, since this scaling is not applied when analyzing displacements [9]. In general, the changes caused by meshing were relatively small, regardless of whether the base shear decreased or increased, remaining within a range of 1% to 6%.

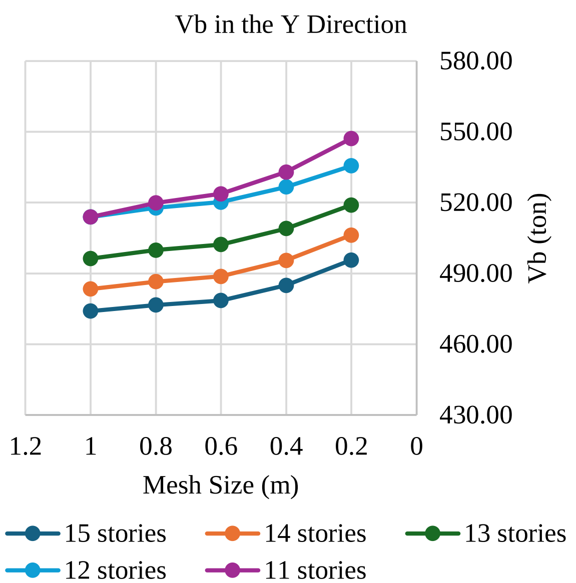

Fig. 10 Base shear in the Y direction according to mesh size for the 15- to 11-story models

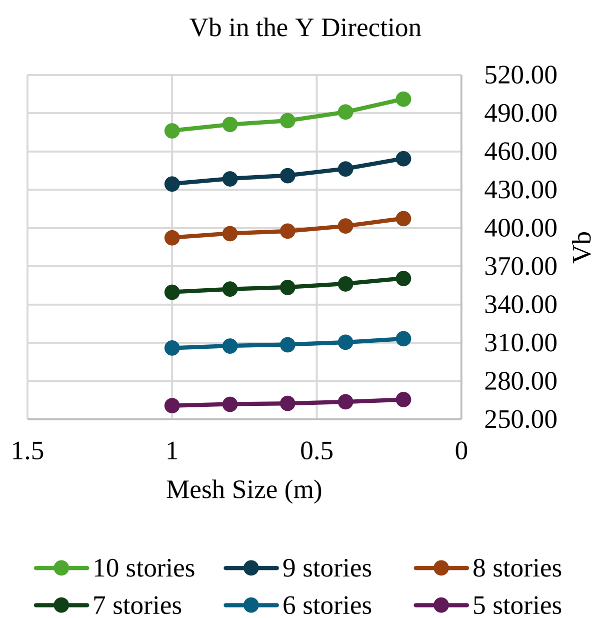

Fig. 11 Base shear in the Y direction according to mesh size for the 10- to 5-story models

3.4. Internal Forces in the Wall

This section presents the results for walls 5 and 7, located along the X and Y directions, respectively, as shown in Figure 12. The analysis of their internal forces was performed using the modal response spectrum results in their corresponding analysis directions. It should be noted that cracking and yielding were not directly simulated in this study, because the analysis was based on a linear modal response spectrum procedure. Therefore, the axial force, shear force, and bending moment results were interpreted as local demand indicators rather than as direct representations of local failure mechanisms.

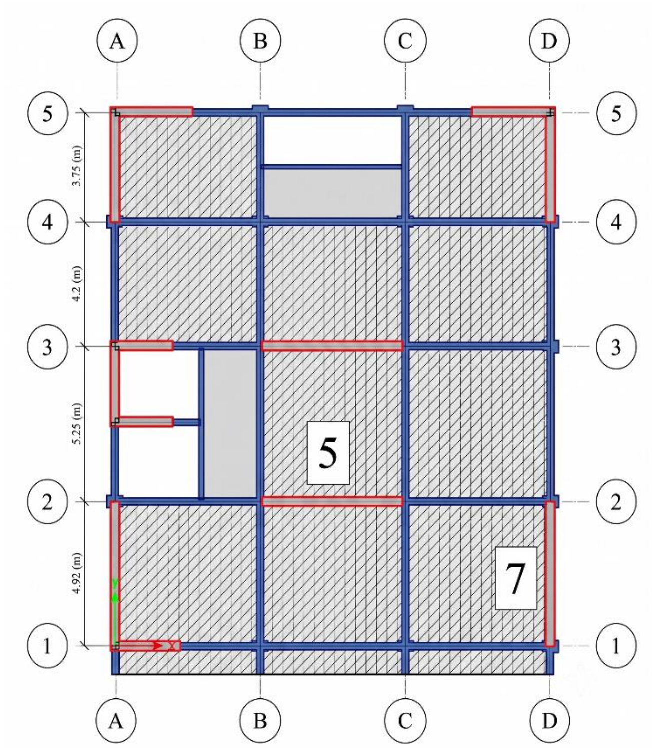

Fig. 12 Location of walls 5 and 7

3.4.1. Axial Force

Table 7. Axial forces, in tons, of wall 5 according to mesh size

Model	1 m	0.8 m	0.6 m	0.4 m	0.2 m
M15	79.83	74.04	71.05	61.42	36.45
M14	73.61	68.19	65.40	56.23	33.41
M13	67.48	62.45	59.87	51.27	30.26
M12	61.37	56.67	54.25	46.23	27.19
M11	55.03	50.72	48.50	41.09	24.12
M10	45.18	42.21	40.78	35.43	21.07
M09	33.62	31.22	30.05	25.90	15.99
M08	23.89	22.04	21.13	18.06	11.08
M07	16.01	14.67	14.00	11.86	7.24
M06	9.95	9.04	8.59	7.22	4.39
M05	5.58	5.03	4.76	3.96	2.41

Table 7 presents the axial force results for all the analyzed models for wall 5, with variations according to mesh size. In all the analyzed models, the greatest variation occurs between the 0.4 m and 0.2 m meshes. However, meshing did not have a substantial effect on the models of different heights, since the variation between the 0.2 m and 1 m meshes remained relatively constant. These variations ranged from 52.45% to 56.17% across all cases.

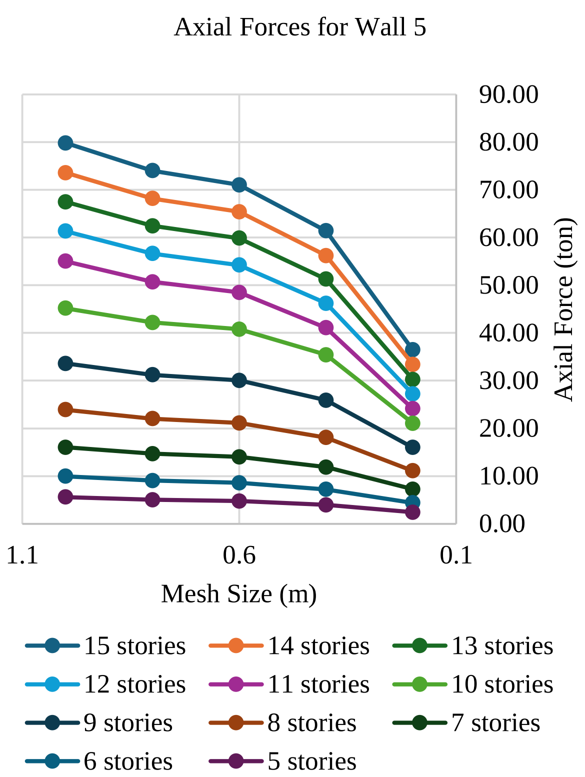

Fig. 13 Axial forces by model and mesh size for wall 5

For wall 7, the axial forces are presented in Table 8 for each mesh size. The variations in the forces between the 0.2 m mesh and the 1 m mesh were smaller, ranging from 9.70% to 18.91%.

Table 8. Axial forces, in tons, of wall 7 according to mesh size

Model	1 m	0.8 m	0.6 m	0.4 m	0.2 m
M15	60.24	60.72	60.76	59.74	54.40
M14	55.33	55.39	55.20	53.83	48.64
M13	50.27	49.97	49.59	47.96	43.04
M12	45.06	44.47	43.95	42.20	37.64
M11	37.50	37.08	36.70	35.34	31.83
M10	27.98	27.53	27.17	26.07	23.38
M09	20.01	19.58	19.27	18.40	16.49
M08	13.61	13.26	13.03	12.40	11.09
M07	8.70	8.46	8.30	7.89	7.06
M06	5.15	5.00	4.91	4.66	4.18
M05	2.76	2.68	2.63	2.51	2.26

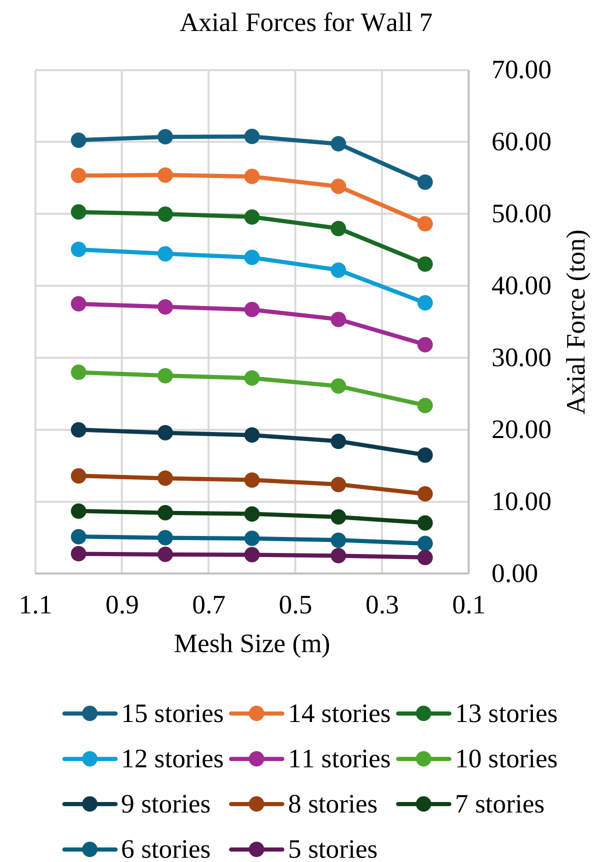

Fig. 14 Axial forces by model and mesh size for wall 7

3.4.2. Shear Force

Table 9 presents the shear forces for wall 5 according to the adopted mesh sizes. These variations were smaller than those of the axial force, ranging from 2.50% to 5.53% when comparing the 0.2 m mesh with the 1 m mesh. On the other hand, since this force represents part of the base shear resisted by wall 5, it exhibits the same behavior in the X direction: a decrease in shear for the 11- to 15-story models and an increase for the 5- to 10-story models as the mesh size is reduced, as shown in Figure 15.

Table 9. Shear forces, in tons, of wall 5 according to mesh size

Model	1 m	0.8 m	0.6 m	0.4 m	0.2 m
M15	133.80	133.05	132.52	131.89	128.57
M14	135.63	134.86	134.26	133.25	130.01
M13	138.27	137.56	136.95	135.78	131.80
M12	141.84	141.14	140.48	139.07	134.72
M11	145.56	145.21	144.63	143.13	138.65
M10	140.70	142.61	143.66	146.16	143.86
M09	127.97	129.54	130.37	132.33	135.04
M08	115.11	116.34	116.97	118.45	120.50
M07	102.03	102.94	103.40	104.47	105.97
M06	88.66	89.32	89.63	90.38	91.44
M05	74.96	75.41	75.62	76.12	76.83

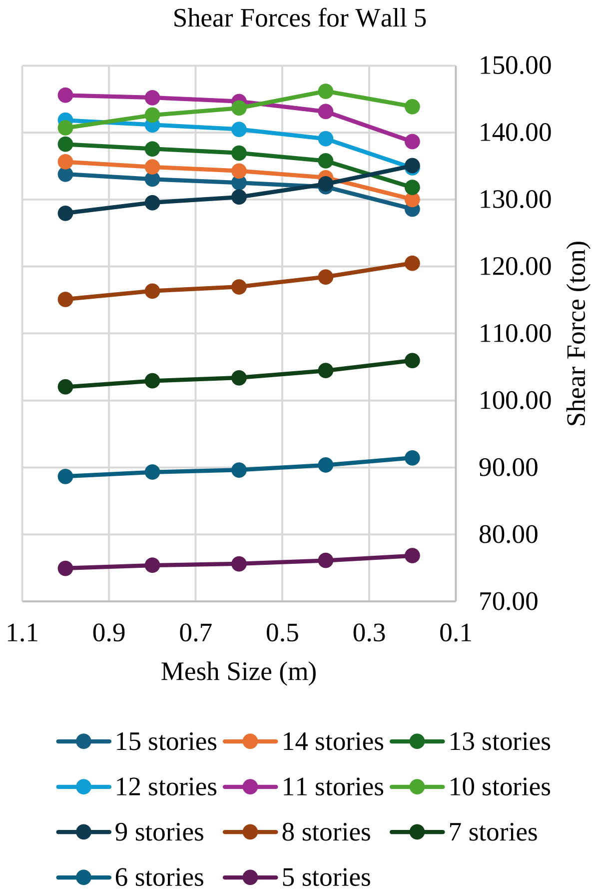

Fig. 15 Shear forces by model and mesh size for wall 5

Table 10 shows the shear force results for wall 7, with variations between the 0.2 m and 1 m meshes ranging from 7.14% to 12.41%. For all models, a decrease is observed as the mesh is refined, as shown in Figure 16. However, an increase would be expected, since the base shear in the Y direction increases as the mesh size is reduced. Nevertheless, because this element resists only part of the base shear, the demand may be redistributed toward other, stiffer elements, causing its shear force to decrease.

Table 10. Shear forces, in tons, of wall 7 according to mesh size

Model	1 m	0.8 m	0.6 m	0.4 m	0.2 m
M15	131.39	126.85	123.64	120.18	115.09
M14	133.72	129.37	126.26	122.95	117.89
M13	137.08	132.92	129.89	126.69	121.50
M12	141.79	137.79	134.80	131.61	126.22
M11	142.23	138.92	136.40	134.02	130.02
M10	132.34	129.44	127.17	124.78	120.53
M09	120.82	118.38	116.44	114.35	110.63
M08	109.31	107.25	105.60	103.75	100.44
M07	97.67	95.92	94.53	92.91	90.02
M06	85.73	84.27	83.12	81.73	79.28
M05	73.36	72.17	71.25	70.11	68.12

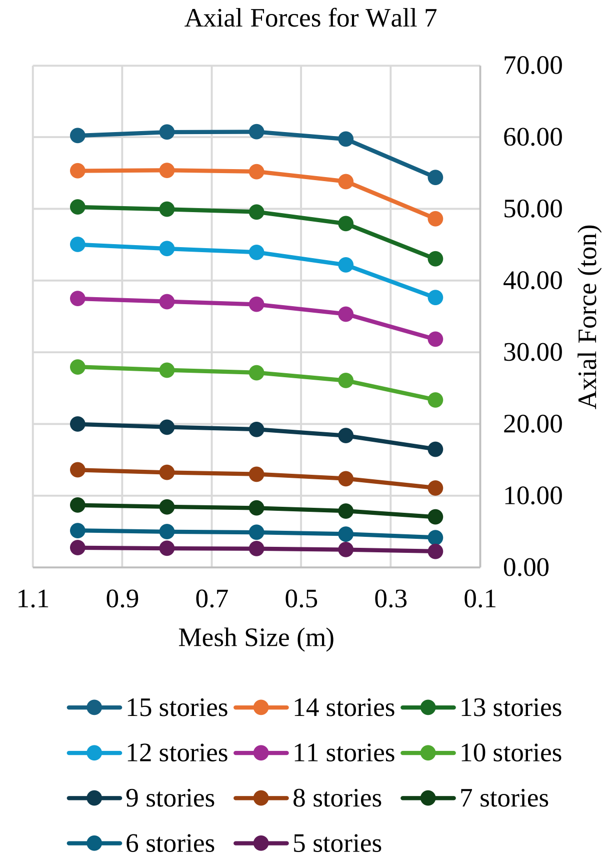

Fig. 16 Shear forces by model and mesh size for wall 7

3.4.3. Bending Moment

Table 11 shows the bending moment results for wall 5 for each model. According to Figure 17, the moments tend to increase as the mesh size is reduced. However, for the 10- to 15-story models, the difference in moments with respect to height was minimal. From the 10-story model onward, the difference was notable; furthermore, in all cases, as the mesh size decreased, the moment values tended to increase. The variations in the results for the 0.2 m mesh relative to the 1 m mesh ranged from 11.33% to 22.39%.

Table 11. Bending moments, in ton·m, of wall 5 according to mesh size

Model	1 m	0.8 m	0.6 m	0.4 m	0.2 m
M15	1872.04	1904.82	1928.61	1996.04	2115.02
M14	1874.68	1907.46	1930.12	1991.18	2112.78
M13	1883.59	1917.75	1940.52	1999.36	2108.50
M12	1898.50	1933.04	1955.26	2010.56	2113.62
M11	1906.82	1945.50	1968.57	2021.81	2121.40
M10	1785.04	1851.31	1895.18	2002.80	2130.82
M09	1552.93	1606.73	1641.97	1727.36	1900.58
M08	1323.19	1364.99	1392.10	1457.08	1586.81
M07	1096.30	1127.09	1146.87	1193.71	1285.38
M06	874.16	895.35	908.79	940.22	1000.12
M05	660.45	673.75	682.04	701.13	736.30

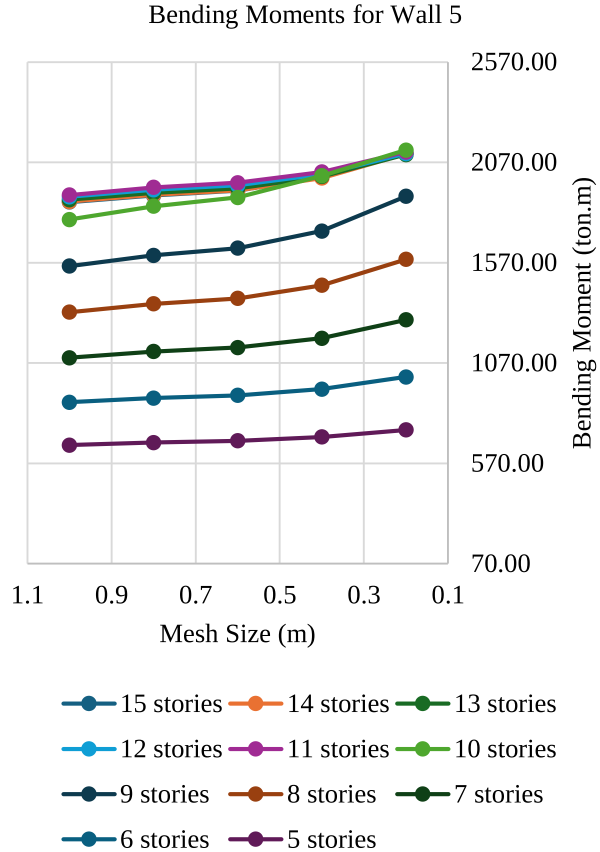

Fig. 17 Bending moments by model and mesh size for wall 5

The results for wall 7 are presented in Table 12, and Figure 18 shows the trend in bending moments as the mesh size is reduced. This element follows the same relationship as wall 5, since smaller differences are observed for the 11- to 15-story models. In this case, there was neither a consistent reduction nor a consistent increase as the mesh was refined, but rather a combination of both: the values decreased up to a mesh size of 0.6 m and then increased as the mesh size was reduced from 0.6 m to 0.2 m.

Table 12. Bending moments, in ton·m, of wall 7 according to mesh size

Model	1 m	0.8 m	0.6 m	0.4 m	0.2 m
M15	1201.62	1186.29	1179.96	1188.81	1230.34
M14	1198.23	1185.16	1180.13	1191.02	1232.58
M13	1198.39	1187.57	1183.61	1195.60	1234.90
M12	1202.56	1193.35	1189.96	1202.03	1237.97
M11	1158.28	1153.71	1153.51	1171.06	1216.95
M10	1018.70	1013.99	1012.71	1023.93	1052.83
M09	868.10	863.48	861.72	869.45	890.74
M08	724.35	719.22	716.81	721.14	734.63
M07	587.66	581.85	578.82	580.23	587.42
M06	458.96	452.67	449.24	448.44	450.99
M05	340.00	333.68	330.17	328.02	327.57

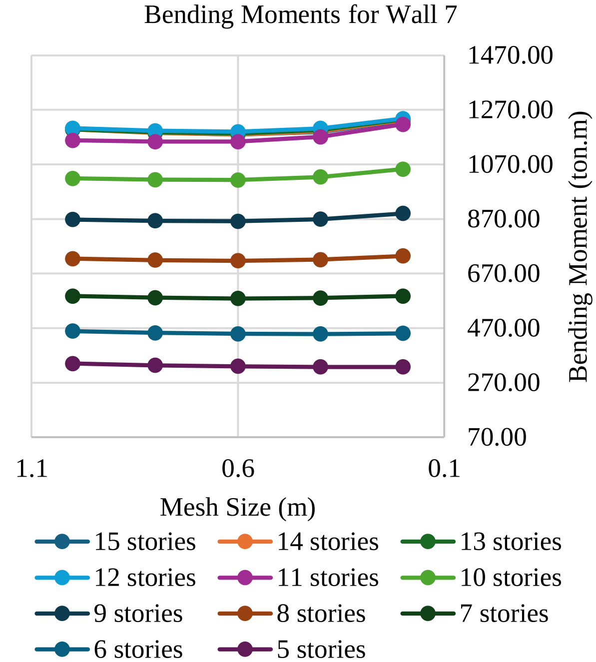

Fig. 18 Bending moments by model and mesh size for wall 7

In general, for each wall, these changes in internal forces caused by mesh refinement can be related to a better distribution of internal stresses. Smaller elements provide a more detailed representation of wall deformation and its interaction with the structural system, thereby avoiding excessive stress concentrations that may occur when a coarser mesh size is used.

4. Conclusion

The present study shows that the mesh size considered for wall modeling in ETABS directly influences the seismic response and that the results also vary according to building height. As the mesh size decreases, interstory drifts and vibration periods progressively increase, thereby representing a more flexible structure. Among the mesh sizes considered, relatively small changes are observed for 1 m, 0.8 m, and 0.6 m, whereas greater variations occur for mesh sizes of 0.4 m and 0.2 m.

Meshing does not produce uniform changes across all the analyzed models; rather, the results vary with height. The taller models were the most sensitive to changes in meshing, especially for a mesh size of 0.2 m. According to the analysis, the drift variations between the 0.2 m mesh and the 1 m mesh for the 15-story model were 37.81% in the X direction and 17.05% in the Y direction, whereas in the 5-story model, they were smaller, at 11.06% and 4.83%, respectively. In this sense, mesh size becomes a more influential factor in the results for medium- and high-rise buildings, particularly in the analysis direction in which the structure shows greater sensitivity to stiffness changes.

The vibration periods also increased as the mesh size decreased; in this case, the variations were more uniform, since they became smaller as the number of stories decreased. For the 15-story model, the variation between the 0.2 m and 1 m meshes was 14.19% for mode 1, 4.80% for mode 2, and 7.20% for mode 3, whereas for the 5-story model, the variations were 6.70%, 1.24%, and 2.63%, respectively.

The sensitivity of the results in each direction is not proportional. This indicates that, in addition to meshing, the stiffness distribution is also conditioned by the arrangement of the walls and the presence of torsion. As a result, despite using the same mesh size, proportional results are not obtained in both directions.

The base shear showed smaller variations, similar to those observed for the periods, ranging between 1% and 6%. However, its behavior was not uniform as the mesh was refined. A decrease in shear was observed in the X direction for the 11- to 15-story models, whereas in the 5- to 10-story models it tended to increase. In the Y direction, an increase was observed in all models.

Regarding the internal forces in the walls, axial forces and bending moments showed the greatest variations as the mesh size was reduced. In wall 5, the variations reached up to 56.17%, whereas in wall 7, they reached up to 18.91%. The bending moments in wall 5 showed variations between 11.33% and 22.39%; in contrast, in wall 7, they were less uniform, showing reductions up to a mesh size of 0.6 m and a subsequent increase toward 0.2 m. The shear forces showed variations between 2.50% and 5.53% for wall 5, whereas for wall 7, they ranged from 7.14% to 12.41%. Based on these results, it is suggested that mesh refinement not only increases the magnitudes, but that its behavior also depends on how the forces are redistributed among the different walls of the Building.

The results allow concluding that the selection of a mesh size should be adopted according to the conditions of the structural type. In buildings dominated by walls and with a greater number of stories, a coarse mesh may slightly overestimate deformations and internal force demands. In particular, greater care should be taken with interstory drifts, since Standard E.030 establishes a limit for this parameter, which may be exceeded depending on the mesh size considered for the analysis. This study also demonstrates the relationship between building height and mesh size, since smaller mesh sizes lead to greater sensitivity, especially as the building height increases.

When defining the mesh size of shear walls in structural analysis, the change that it may have should be verified by making comparisons between the results, since these may vary, especially in interstory drifts, making the structure more flexible, even more so in directions where there is lower stiffness. The greatest differences were presented with meshes from 0.6 m to 0.2 m with respect to the 1 m mesh, so a size within this range could be considered, although with a size of 0.2 m and depending on the complexity of the model, it could require more computational time. This study focused on linear analysis, but the effect of these could also be addressed in the future in nonlinear analyses through pushover or nonlinear time-history analysis. In addition, the behavior in irregular buildings could be evaluated, and it could be identified which ones are more variable to mesh sensitivity.

References

[1] Erick A. Burgos, and Edgar Orlando Sigüenza, *Modeling Structures with ETABS*, Antiguo Cuscatlán, La Libertad, El Salvador: UCA Academic Publications, 2022. [Google Scholar] [Publisher Link]

[2] Deyvid Froilán Matamoros Paitán et al., "Influence of Structural Properties Modeling in Building Analysis: Diaphragms, Rigid-Zone Factor and Wall Meshing," *Civil Engineering and Architecture*, vol. 12, no. 3, pp. 1593-1610, 2024. [CrossRef] [Google Scholar] [Publisher Link]

[3] Pernaty Ramu, S. M. Abdul Mannan Hussain, and B. Tharun Kumar, "Design and Analysis of Precast Load Bearing Walls for Multi Storey Building Using Etabs," *International Journal of Modern Engineering Research*, vol. 4, no. 7, pp. 6-13, 2014. [Google Scholar] [Publisher Link]

[4] Ovidiu Chelariu, Ioan-Petru Ciongradi, and Mihai Budescu, "Errors in Concrete Shear Wall Elastic Structural Modeling," *Bulletin of the Polytechnic Institute of Iaşi, Section Construction. Architecture*, vol. 57, no. 2, pp. 41-49, 2011. [Google Scholar]

[5] Aldi Rusi, "*Comparison of Different Approaches for Shearwall Modelling*," M.S. Thesis, Faculty of Architecture and Engineering, Epoka University, pp. 1-92, 2014. [Google Scholar] [Publisher Link]

[6] Joe Mangan, "*Modal Analysis of Cal Poly's Kennedy Library Using Computational Modeling*," California Polytechnic State University, pp. 1-47, 2025. [Google Scholar] [Publisher Link]

[7] G. Juárez-Luna, and P. Ortiz Gálvez, "Importance of Meshing Finite Elements of Confined Masonry Walls in the Seismic Analysis of Buildings," *International Journal of Structural Engineering*, vol. 26, no. 4, pp. 712–745, 2021. [Google Scholar]

[8] Derek A. Skolnik, John W. Wallace, "Critical Assessment of Interstory Drift Measurements," *Journal of Structural Engineering*, vol. 136, no. 12, 2010. [CrossRef] [Google Scholar] [Publisher Link]

[9] Ministry of Housing, Construction and Sanitation, Technical Standard E.030: Ermanent Technical Committee NTE E-030 Earthquake Resistant Design, 2020. [Online]. Available: https://iisee.kenken.go.jp/worldlist/42_Peru/TechnicalStandardOfBuilding_E.030_ENG_2018.pdf

[10] J. W. Tedesco, and T. Krauthammer, *Structural Dynamics, Structural Engineering and Geomechanics*, vol. 2, pp. 1-12, 2000. [Google Scholar] [Publisher Link]

[11] Jack P. Moehle et al., "Seismic Design of Cast-in-Place Concrete Special Structural Walls and Coupling Beams: A Guide for Practicing Engineers," *NEHRP Seismic Design Technical Brief*, pp. 1-41, 2011. [Google Scholar] [Publisher Link]

[12] Finley A. Charney, *Reinforced Concrete*, NEHRP Recommended Provisions: Design Examples, FEMA 451, Federal Emergency Management Agency, 2006. [Google Scholar] [Publisher Link]

[13] J. Tarigan, J. Manggala, and T. Sitorus, "The Effect of Shear Wall Location in Resisting Earthquake," *IOP Conference Series: Materials Science and Engineering*, vol. 309, pp. 1-7, 2018. [CrossRef] [Google Scholar] [Publisher Link]

[14] Prashidha Khatiwad, and Elisa Lumantarna, "Simplified Method of Determining Torsional Stability of the Multi-Storey Reinforced Concrete Buildings," *CivilEng*, vol. 2, no. 2, pp. 290-308, 2021. [CrossRef] [Google Scholar] [Publisher Link]

[15] Mir M. Ali, and Kyoung Sun Moon, "Advances in Structural Systems for Tall Buildings: Emerging Developments for Contemporary Urban Giants," *Buildings*, vol. 8, no. 8, pp. 1-34, 2018. [CrossRef] [Google Scholar] [Publisher Link]

[16] Can Balkaya, and Erol Kalkan, "Estimation of Fundamental Periods of Shear-Wall Dominant Building Structures," *Earthquake Engineering and Structural Dynamics*, vol. 32, no. 7, pp. 985-998, 2003. [CrossRef] [Google Scholar] [Publisher Link]

[17] Talha Polat Doğan, and Ibrahim Hakkı Erkan, "Evaluation of the Nonlinear Seismic Responses of High-Rise Reinforced Concrete Buildings with Different Foundations and Structural Plans - Considering Soil-Structure Interactions," *Buildings*, vol. 14, no. 6, pp. 1-21, 2024. [CrossRef] [Google Scholar] [Publisher Link]